Effects of Dietary Calcium on *Helicobacter pylori*-induced Gastritis in Mongolian Gerbils

MASAKI IIMURO[1], SHIRO NAKAMURA[1], TETSUO ARAKAWA[2], KEIJI WAKABAYASHI[3] and MICHIHIRO MUTOH[4]

[1]*Department of Lower Gastroenterology, Hyogo College of Medicine, Hyogo, Japan;*
[2]*Department of Gastroenterology, Graduate School of Medicine, Osaka City University, Osaka, Japan;*
[3]*Institute for Environmental Sciences, University of Shizuoka, Shizuoka, Japan;*
[4]*Division of Cancer Prevention Research, National Cancer Center Research Institute, Tokyo, Japan*

Abstract. *Background and Aims: Helicobacter pylori (Hp) infection causes gastritis and is considered a gastric cancer risk factor. We have previously reported that codfish meal markedly enhanced Hp-induced gastritis in Mongolian gerbils. In the present study, we sought the responsible components in codfish meal. Materials and Methods: Codfish were divided into three parts (meat, viscera and 'other parts', including bone), and administered to Hp-infected gerbils. Subsequently, cod bone, sardine bone and prawn shell were tested, along with major calcium components, hydroxyapatite and calcium carbonate, in bone and shell, respectively. Results: 'Other parts' and cod bone enhanced Hp-induced gastritis, as was observed for whole codfish. Similarly, sardine bone and prawn shell, as well as 0.22-0.88% hydroxyapatite and calcium carbonate, enhanced gastritis. In contrast, administration of a higher dose of the calcium compounds exerted protective effects. Conclusion: Intake of calcium compounds may contribute to enhancement of Hp-induced gastritis.*

Gastric cancer continues to be one of the most common malignancies in Japan and many other countries. Gastiric cancer risk is known to be associated with *Helicobacter pylori* (*Hp*) infection, a high intake of salty foods and an insufficient intake of fresh fruits and vegetables (1). Since half of the world's population is believed to be infected with *Hp* (2), control of *Hp*-induced disorders may lead to prevention of gastric cancer development (3-5).

Correspondence to: Michihiro Mutoh, Division of Cancer Prevention Research, National Cancer Center Research Institute, 1-1, Tsukiji 5-chome, Chuo-ku, Tokyo 104-0045, Japan. Tel: +81 335422511 ext 4351, Fax: +81 335439305, e-mail: mimutoh@ncc.go.jp

Key Words: Gastritis, *Helicobacter pylori*, fish meal, calcium, Mongolian gerbils.

Mongolian gerbils (*Meriones unguiculatus*) can readily be colonized by *Hp*, subsequently demonstrating chronic gastritis, gastric ulcers and intestinal metaplasia (6, 7). Moreover, it has been reported that *Hp* infection plus treatment with chemical carcinogens, *N*-methyl-*N*-nitrosourea (MNU) or *N*-methyl-*N'*-nitro-*N*-nitrosoguanidine, can induce gastric cancer in Mongolian gerbils, with pathological changes similar to those observed in humans (8-10). Additional treatment with 2.5-10% sodium chloride in the diet has been also reported to enhance gastric carcinogenesis in *Hp*-infected and MNU-treated Mongolian gerbils (11). Recently, a combination of 1-nitrosoindole-3-acetonitrile administration and *Hp* infection was shown to cause gastric cancer in Mongolian gerbils (12).

By using Mongolian gerbils, we have provided evidence that fish meal in conventional diets notably enhances *Hp*-induced gastritis as compared to a diet without fish meal, without any apparent major effect on numbers of *Hp* (13). However, fish meal has not yet been reported as being a risk factor for gastritis and gastric cancer. Of note, in the previous study, almost the same numbers of *Hp* were cultured from the gastric mucosa in both dietary groups (13). It has been suggested that *Hp*-induced gastritis and ulceration are influenced by both the *Hp* strain and host defensive factors. Furthermore, the potential for host defense may be affected by dietary habits (14, 15). However, risk factors regarding dietary habits for gastritis are not fully-understood, except for the case of high intake of salty foods. Thus, it is important to elucidate the components in fish meal that enhance *Hp*-induced gastritis and may thus be linked to *Hp*-related gastric carcinogenesis. Therefore, in the present study, we explored the effects of different components of fish meal and demonstrated that calcium intake in fish meal can affect *Hp*-induced gastritis in Mongolian gerbils.

Materials and Methods

Animals and chemicals. Six-week-old, specific pathogen-free male Mongolian gerbils were purchased from Seac Yoshitomi, Ltd.

(Fukuoka, Japan), and housed in polycarbonate cages on wood chip bedding in an air-conditioned biohazard room with a 12-h light/dark cycle. They were given a basal diet and water *ad libitum* until the start of the experiment. We purchased the ingredients for the conventional diet and AIN-76A from Nippon Formula Feed Manufacturing Co., Ltd. (Tokyo, Japan). Hydroxyapatite, calcium carbonate and calcium hydrogenphosphate dihydrate were purchased from Wako Pure Chemical Industries, Ltd. (Osaka, Japan). Raw codfish, sardine and prawn were purchased at Tsukiji Market (Tokyo, Japan), divided, sterilized and freeze-dried.

Preparation of test diets. The basal diet, namely 10% casein diet, was made by replacing fish meal with casein in the conventional diet containing 10% fish meal, as previously reported (13). For preparing test samples, raw codfish was divided into three parts namely meat, viscera, and other parts, including bone, and each part was sterilized, freeze-dried and cut into small pieces. The ratio of weight of meat:viscera:other was 52:3:45, respectively. These three parts were mixed with casein diet to make 5.2% meat with 4.8% casein diet, 0.3% viscera with 9.7% casein diet, and 4.5% other with 5.5% casein diet, according to the freeze-dried weight ratios. Cod bone was isolated from codfish and washed with distilled water, sterilized, freeze-dried and cut into small pieces. It was also mixed with casein diet to make a 2% test diet, because the 'other' diet contained 2% bone in freeze-dried weight. Similarly, small pieces of sardine bone and prawn shell were each blended with casein diet to make 2% test diets. We also prepared a mixture of ingredients of AIN-76A without calcium hydrogenphosphate dihydrate to make a calcium-free basal diet, designated as calcium-free AIN-76A. Hydroxyapatite, calcium carbonate and hydrogenphosphate dihydrate were each blended with this calcium-free AIN-76A to make hydroxyapatite, calcium carbonate and hydrogenphosphate dihydrate diets at concentrations of 0.22, 0.44, 0.88, 1.75 and 3.50%. These two-fold serial doses were used because 1.75% calcium hydrogenphosphate dihydrate is included in the AIN-76A diet.

H. pylori preparation. *Hp* (ATCC 43504; American Type Culture Collection, Rockville, MD, USA) bacteria were grown in brucella broth (BBL, Cockeysville, MD, USA) containing 10% heat-inactivated horse serum (Nacalai Tesque, Kyoto, Japan) for 24 h at 37°C under microaerobic conditions (5% O_2, 10% CO_2, and 85% N_2) on a rotary shaker at 120 rpm, and aliquots (4.0×10^8 CFU/ml) were used as the inoculum for the animal experiments.

Animal experimental design. Seven-week-old Mongolian gerbils were given an intragastric inoculation of the broth culture of *Hp* (0.5 ml, 2.0×10^8 CFU) after fasting for 24 h. As a control group for *Hp* infection, *Hp*-free animals received only sterilized brucella broth instead. Four hours later, all animals were fed *ad libitum* until the end of the experiment. Body weights and diet intakes were measured weekly and the general health of the animals was monitored daily.

After six weeks administration of the test diets, all animals were sacrificed under ether anesthesia at 13 weeks of age. Their stomachs were excised and opened along the greater curvature, and the contents were gently removed by washing with 10 mM phosphate buffered saline (PBS, pH 7.4). Macroscopic gastric lesions, including mucosal thickening and hemorrhage were recorded, and wet weights of the whole stomach, including the forestomach and glandular stomach, were measured. To evaluate the degree of gastric hemorrhage, the number of hemorrhagic spots was counted. Each stomach was divided into two halves, one for histological examination being fixed in 10% neutral buffered formalin, processed for embedding in paraffin and stained with hematoxylin and eosin (H&E). Determination of serum calcium and gastrin levels was performed by radioimmunoassay (RIA) and the arsenazo III method, respectively. Animal studies were performed according to the guidelines for animal experiments at the National Cancer Center.

Culture of Hp. For detection of Hp, mucosal samples of glandular stomach parts were scraped from the remaining stomach halves, homogenized with 0.3 ml PBS and diluted with the same solution. Aliquots (100 μl) of this suspension were inoculated onto segregating agar plates for *Hp* (Nissui Pharmaceutical Co., Ltd., Tokyo, Japan) with incubation at 37°C for five days under microaerobic conditions. Bacterial colonies were identified by the rapid urease test (CLO test; Tri-Med Specialties, Inc., Lenexa, KS, USA) and Gram staining for morphology. Their numbers were then counted.

Statistical analysis. All data were expressed as means±SD. Differences in incidences of gastric lesions between groups were examined for statistical significance using the Fisher's exact test, and those for other data were examined using Welch's *t*-test. $p<0.05$ was considered to be significant.

Results

Whole codfish were divided into three parts (meat, viscera and 'other parts' including fish bone) in order to examine the components responsible for enhancing gastritis in Mongolian gerbils. Administration of each part of the codfish diet did not affect the feeding or other behavior of Mongolian gerbils. No significant differences in body weight were observed among the groups.

In Table I, data for the effects of whole codfish, and the three divided fractions on *Hp*-induced gastric lesions are summarized. In the *Hp*-inoculated group fed whole codfish diet, edematous thickening was observed in the gastric mucosa, especially in the pylorus, in 7 out of 10 animals and hemorrhagic spots in 5 (Figure 1). No visible gastric lesions were observed in the basal control, codfish-meat and viscera-diet groups. On the other hand, in the 'other parts' diet group, enhancing effects similar to those observed in the group fed whole-codfish diet were noted, with edematous thickening being observed in 8 out of 10 animals and hemorrhagic spots in 9 (Figure 1). Along with edema and hemorrhage, both stomach wet weights and the number of hemorrhagic spots per animal increased significantly in groups fed whole codfish and 'other parts' diet, histological examination revealing mononuclear cell and neutrophil infiltration into the submucosal and *lamina propria* layers, and hyperplastic and cystic changes of the glandular epithelium in the pyloric region. *Hp* from all animals was successfully cultured in the all *Hp*-inoculated groups. Average numbers of viable bacteria [log (CFU/stomach)]

Table I. *Fractions of codfish and their effects on H. pylori-induced gastritis in Mongolian gerbils.*

Diet	No. of animals (%) with			No. of colonies of *H. pylori* (log CFUs/ stomach)[a]	Stomach wet weight (g)[a]	No. of hemorrhagic spots/animal[a]	Calcium levels in serum (mg/dl)[a]	Gastrin levels in serum (pg/ml)[a]
	Edema	Hemorrhage	*H. pylori* infection					
Basal	0/10 (0)	0/10 (0)	10/10 (100)	4.2±0.3	0.63±0.04	0	9.2±0.4	220±60
10% Whole codfish	7/10 (70)[b]	5/10 (50)[c]	10/10 (100)	4.1±0.7	0.93±0.24[d]	11.3±12.4[d]	9.3±0.2	320±35
5.2% Meat	0/10 (0)	0/10 (0)	10/10 (100)	4.0±0.2	0.65±0.04	0	9.1±0.4	250±72
0.3% Viscera	0/10 (0)	0/10 (0)	10/10 (100)	4.0±0.3	0.67±0.05[e]	0	9.5±0.3	260±64
4.5% Other parts	8/10 (80)[b]	9/10 (90)[b]	10/10 (100)	3.8±0.9	1.02±0.23[d]	11.9±8.1[d]	9.6±0.3	280±110

Samples were supplemented to basal (fish meal-free) diet. To evaluate the degree of gastric hemorrhage, the number of hemorrhagic spots were counted. [a]Mean±SD. [b]$p<0.01$ and [c]$p<0.05$ *versus* basal diet group by Fisher's exact test; [d]$p<0.01$ and [e]$p<0.05$ *versus* basal diet group by Welch's *t*-test.

Table II. *Effects of fish bones and prawn shell on H. pylori-induced gastritis in Mongolian gerbils.*

Diet	No. of animals (%) with			No. of colonies of *H. pylori* (log CFUs/ stomach)[a]	Stomach wet weight (g)[a]	No. of hemorrhagic spots/animal[a]
	Edema	Hemorrhage	*H. pylori* infection			
Basal	0/10 (0)	2/10 (20)	10/10 (100)	4.5±0.5	0.63±0.06	1.5±3.4
2% Cod bone	9/10 (90)[b]	8/10 (80)[c]	10/10 (100)	4.8±0.7	0.88±0.26[d]	11.7±15.3[e]
2% Sardine bone	6/10 (60)[c]	6/10 (60)	10/10 (100)	4.5±0.7	0.76±0.12[d]	7.8±7.6[e]
2% Prawn shell	7/10 (70)[b]	5/10 (50)	10/10 (100)	5.4±0.5[e]	0.84±0.26[e]	10.8±14.2[e]

Samples were supplemented to basal (fish meal-free) diet. [a]Mean±SD. [b]$p<0.01$ and [c]$p<0.05$ *versus* basal diet group by Fisher's exact test; [d]$p<0.01$ and [e]$p<0.05$ *versus* basal diet group by Welch's *t*-test.

obtained from *Hp*-infected stomach samples are also shown in Table I. No significant differences were observed among the five groups. In the *Hp*-free groups of gerbils, no gastric lesions were detected macroscopically or microscopically. Serum calcium levels ranged between 9.1-9.6 mg/dl and did not change remarkably. Serum gastrin levels tended to be higher in whole codfish and 'other parts' diet-treated animals, but not significantly.

The 'other parts' is diet mainly consisting of cod bone. Therefore, the effect of cod bone on *Hp*-induced gastritis was examined. Administration of a cod bone diet did not affect the feeding or other behavior of the gerbils. No significant differences in body weights were observed compared with the basal control group. Enhancing effects of cod bone diet on *Hp*-induced gastritis were found, as evident in Table II. The number of animals with edema, the stomach wet weights and the number of hemorrhagic spots per animal were increased significantly. No gastric lesions were detected in *Hp*-free gerbils fed the same diet. Histological changes in the glandular stomach of *Hp*- and cod bone-treated animals were the same as those of *Hp*- and whole cod fish- or 'other parts' diet-treated animals.

In addition to cod bone, sardine bone and prawn shell were administered to *Hp*-infected gerbils. As in the case of cod bone, administration of sardine bone and prawn shell diet did not affect the feeding and body weights in the groups studied. As shown in Table II, the number of animals with edema, the stomach wet weights and the number of hemorrhagic spots per animal were again significantly increased with histological changes in the glandular stomach in these groups similar to those in the cod bone-fed group.

Since most calcium in cod and sardine bones comes from hydroxyapatite and the one in prawn shell is calcium carbonate, calcium-free AIN-76A diet was supplemented with these calcium compounds at 0.22 to 3.50%. Administration of these diets did not affect the feeding or other behavior of the gerbils but effects were noted on *Hp*-induced gastritis (Table III). Among the calcium-administered groups, hydroxyapatite enhanced *Hp*-induced gastritis. The stomach wet weights and the number of hemorrhagic spots per animal were increased significantly by 0.88 and 1.75% doses of hydroxyapatite. However, in the 3.50% hydroxyapatite group, 3 out of five animals were not infected with *Hp* at the end of the experiment, and were free

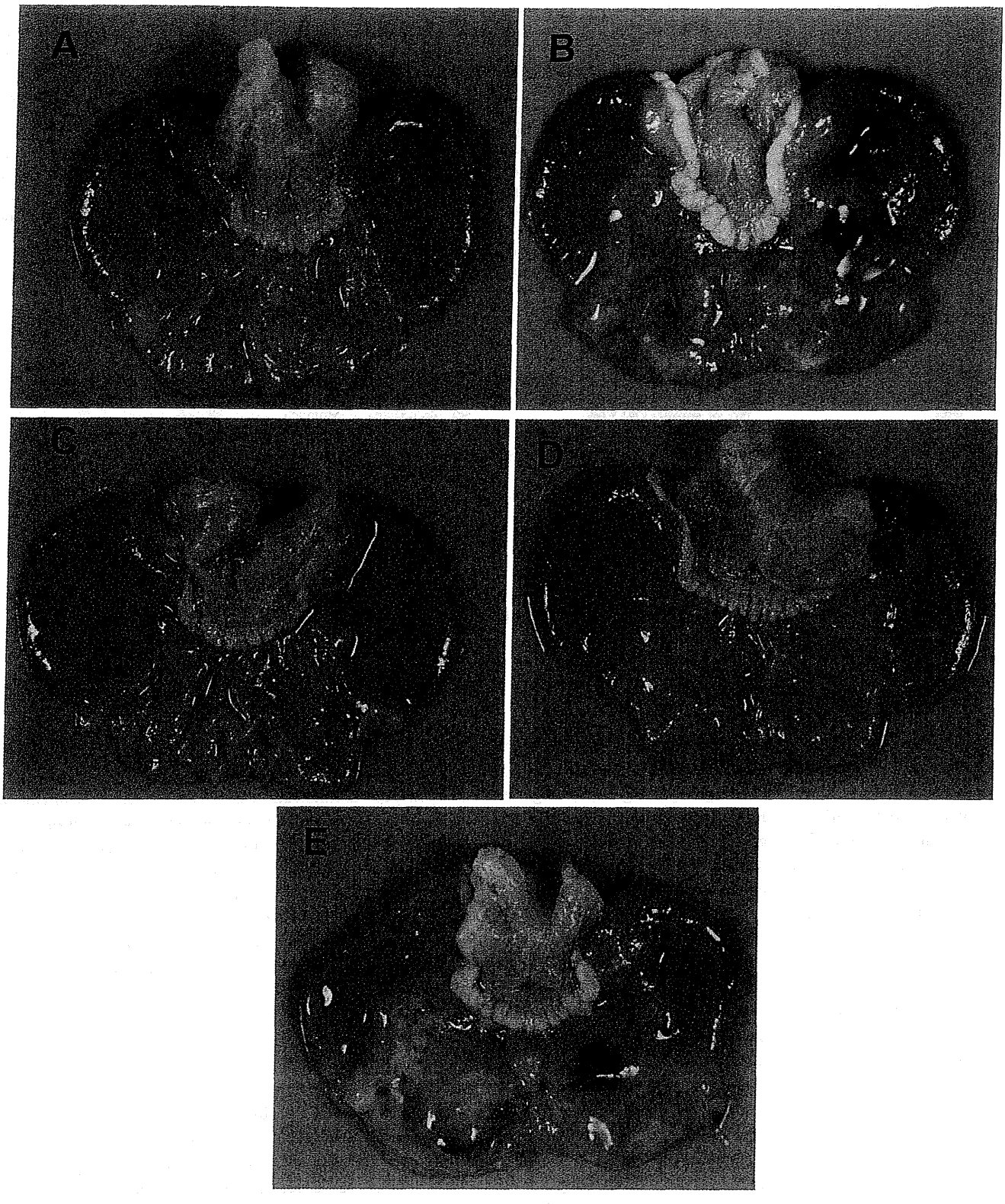

Figure 1. *Typical macroscopic views of glandular stomach of Mongolian gerbils inoculated with Helicobacter pylori (Hp). Treatments: A: 10% Casein basal diet with Hp infection; B: 10% fish meal diet with Hp infection; C: 5.2% meat diet with Hp infection; D: 0.3% viscera diet with Hp infection; E: 4.5% 'other parts' diet with Hp infection.*

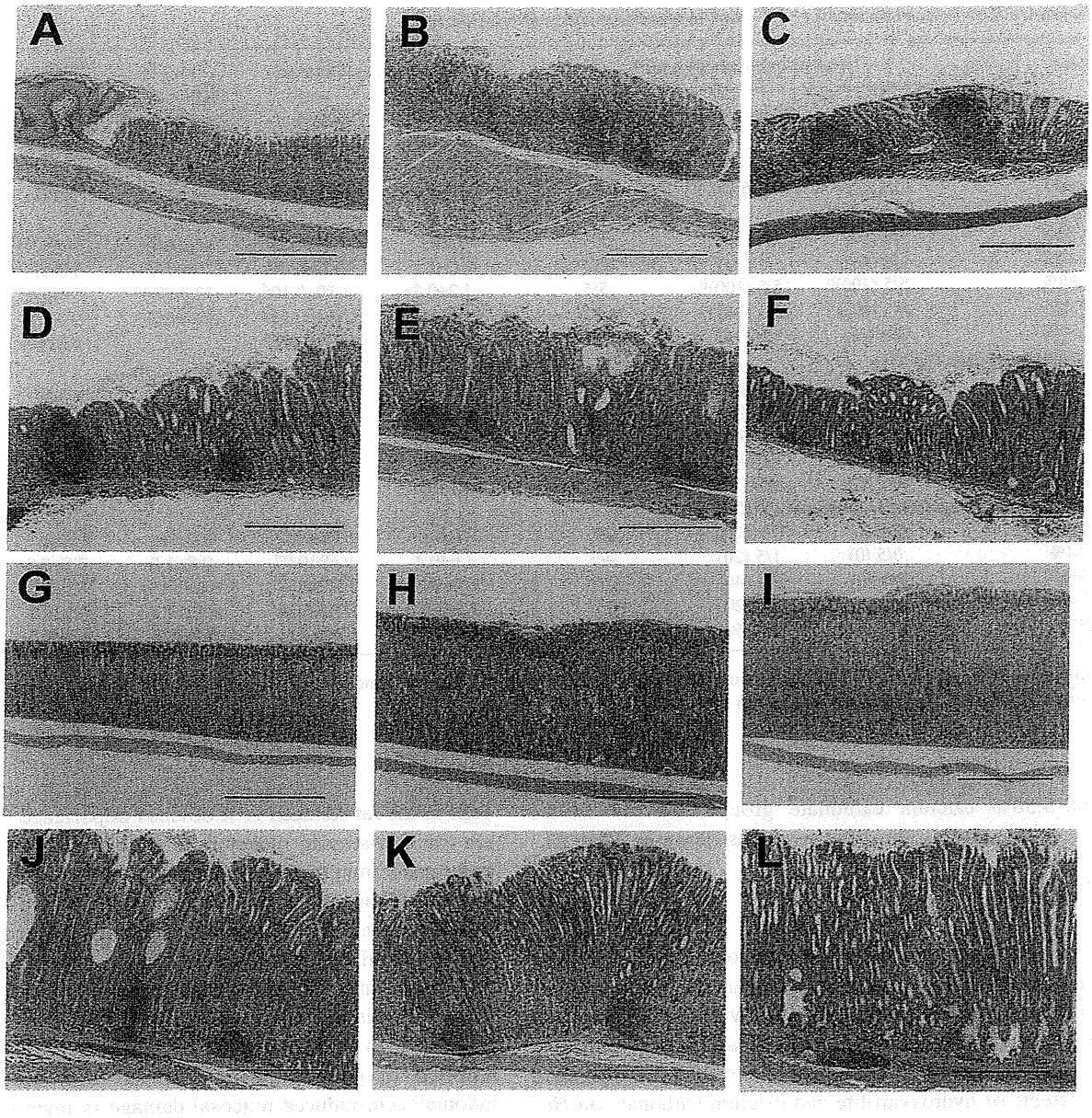

Figure 2. *Typical microscopic views of glandular stomach of Mongolian gerbils without or inoculated with Helicobacter pylori (Hp). Histological findings of sections stained with hematoxylin and eosin of fundic (A-F) and pyloric (G-L) mucosa are presented in the groups treated with 2% cod bone with Hp (C and I), 1.75% hydroxyapatite [$Ca_{10}(PO_4)_6(OH)_2$] with Hp (D and J), 1.75% calcium carbonate ($CaCO_3$) with Hp (E and K), 1.75% calcium hydrogenphosphate dihydrate ($CaHPO_4$) with Hp (F and L). Basal diet groups were inoculated with Hp (B and H) or were without Hp (A and G) and are also shown. Bar=500 μm.*

from gastric hemorrhage, with reduced stomach wet weights. Calcium carbonate had enhancing effects on *Hp*-induced gastritis involving edema and hemorrhage. The stomach wet weights and the number of hemorrhagic spots per animal were increased significantly in the 0.88% calcium carbonate group. However, in the 3.50% calcium carbonate group, stomach wet weights and the numbers of hemorrhagic spots were lower than those in the 0.88% group. In addition, weak, but not statistically significant, enhancing effects on gastritis were observed in the calcium hydrogenphosphate dihydrate groups. Histological changes in the glandular stomach in hydroxyapatite and calcium carbonate groups were similar to those in cod bone- and prawn shell-fed groups, respectively (Figure 2). Serum calcium levels ranged from 9.1-9.9 mg/dl, and were not remarkably changed. Serum gastrin levels were higher in the 1.75% hydroxyapatite and

Table III. *Effects of calcium intake on H. pylori-induced gastritis in Mongolian gerbils.*

Diet	No. of animals (%) with			No. of colonies of *H. pylori* (log CFUs/ stomach)[a]	Stomach wet weight (g)[a]	No. of hemorrhagic spots/animal[a]	Calcium levels in serum (mg/dl)[a]	Gastrin levels in serum (pg/ml)[a]
	Edema	Hemorrhage	*H. pylori* infection					
Basal	0/5 (0)	0/5 (0)	4/5	3.1±0.9	0.67±0.04	0	9.2±0.3	177±6
Hydroxyapatite, $Ca_{10}(PO_4)_6(OH)_2$								
0.22%	3/5 (60)	3/5 (60)	5/5	4.0±0.7	0.89±0.22[e]	4.2±6.7	9.1±0.9	168±78[e]
0.44%	2/5 (40)	1/5 (20)	4/5	4.1±0.5	0.72±0.18	7.0±15.7	9.9±0.2	177±35
0.88%	5/5 (100)[b]	5/5 (100)[b]	5/5	4.2±0.3e	1.19±0.10[d]	12.0±5.4[d]	9.5±0.5	173±32
1.75%	5/5 (100)[b]	5/5 (100)[b]	5/5	4.5±0.3e	1.19±0.13[d]	14.8±5.3[d]	9.4±0.6	277±51[e]
3.50%	0/5 (0)	0/5 (0)	2/5	3.7±0.1	0.53±0.06[d]	0	9.6±0.4	263±31
Calcium carbonate, $CaCO_3$								
0.22%	1/5 (20)	1/5 (20)	5/5	3.9±0.6	0.81±0.17	3.0±6.7	9.4±0.4	170±10
0.44%	2/5 (40)	2/5 (40)	5/5	3.7±0.7	0.88±0.36	6.0±11.3	9.3±0.3	193±32
0.88%	4/5 (80)[c]	4/5 (80)[c]	5/5	4.7±0.7e	0.94±0.23[e]	7.2±7.3[e]	9.4±0.1	227±72[e]
1.75%	3/5 (60)	3/5 (60)	5/5	4.0±0.7	0.86±0.31	12.0±15.6	9.7±0.3	263±105[d]
3.50%	1/5 (20)	1/5 (20)	4/5	4.1±0.4	0.72±0.24	5.2±11.6	9.8±0.6	243±65[e]
Calcium hydrogenphosphate dihydrate, $CaHPO_4 \cdot 2H_2O$								
0.22%	0/5 (0)	1/5 (20)	4/5	3.7±0.5	0.71±0.07	0.2±0.4	9.6±0.3	175±7
0.44%	0/5 (0)	1/5 (20)	4/5	3.6±0.4	0.69±0.07	0.8±1.8	9.8±0.3	180±10
0.88%	1/5 (20)	2/5 (40)	5/5	3.4±1.1	0.77±0.31	6.8±13.6	9.5±0.5	177±25
1.75%	1/5 (20)	1/5 (20)	5/5	3.3±1.2	0.71±0.34	8.4±18.8	9.5±0.2	197±23
3.50%	2/5 (40)	3/5 (60)	5/5	3.7±0.6	0.79±0.31	5.8±8.0	9.8±0.5	193±23

Samples were supplemented to basal (calcium-free AIN-76A) diet. [a]Mean±SD. [b]$p<0.01$ and [c]$p<0.05$ *versus* basal diet group by Fisher's exact test; [d]$p<0.01$ and [e]$p<0.05$ *versus* basal diet group by Welch's *t*-test.

0.88-3.50% calcium carbonate groups, but not in the hydrogenphosphate dihydrate group, as shown in Table III.

Discussion

In the present study, we found that cod bone in fish meal enhanced *Hp*-induced gastritis in Mongolian gerbils and that a similar enhancement was observed with sardine bone and prawn shell administration. To clarify the causative constituents in the fish bones and prawn shell, we examined the effects of hydroxyapatite and calcium carbonate on *Hp*-induced gastritis, and found that both constituents clearly enhanced *Hp*-induced gastritis when fed at 0.22-1.75% in the diet. However, a high dose intake of these compounds (3.5%) resulted in a reduced occurrence of *Hp*-induced gastritis. Calcium hydrogenphosphate dihydrate, included in the AIN-76A diet, also had a weak enhancing effect, but this was not statistically significant.

Several *in vivo* and *in vitro* studies have implied that calcium enhances gastric disorders (16-19). To our knowledge, this is the first report of direct evidence showing that administration of calcium compounds enhances *Hp*-induced gastritis in Mongolian gerbils. Over-secretion of acid (HCl) and loss of feedback control causes gastritis and ulceration. Therefore, the fact that that elevation of extracellular calcium can induce acid secretion from parietal cells in the rat stomach is of obvious importance (16). There are calcium-sensing receptors in G cells and parietal cells, and signals from these receptors play important roles in both acid secretion and mucosal repair (16). Calcium chloride is reported to increase the activity of ornithine decarboxylase and to stimulate DNA synthesis in the pyloric mucosa in F344 male rats (17). In contrast, calcium channel blockers, which inhibit the entry of calcium into cells, attenuate gastritis (18). Calcium channel blockers have been also reported to protect gastric mucosa from ethanol- and indomethacin-induced mucosal damage in male Fisher 344 rats (19). The available data thus suggest that gastritis, gastric ulceration and gastric carcinogenesis might be enhanced by calcium influx. We measured serum calcium levels and gastrin levels as factors responsible for inducing gastric erosion or ulceration by hypergastrinemia and high acid secretion. However, serum calcium levels and gastrin levels did not significantly differ between the gerbils fed basal diet and those fed 10% whole codfish or 'other parts'. Moreover, serum gastrin levels tended to correlate with the amount of hydroxyapatite and calcium carbonate consumption, but not with that of calcium hydrogenphosphate dihydrate. Serum calcium levels and gastrin levels, which may affect gastric pH, may have the same effect on gastritis observed in the present study, but other mechanisms are also suggested to be responsible.

However, epidemiological and experimental studies have demonstrated suppressive effects of calcium intake on gastric cancer development. For example, a case-control study demonstrated gastric cancer risk to be reduced by dietary intake of calcium, carotene, fresh vegetables, fruits and vitamin C (20). One *in vivo* study demonstrated that calcium chloride can inhibit sodium chloride-induced replicative DNA synthesis in the pyloric mucosa of male Fischer 344 rats (21).

In the present study, our data demonstrated enhancing and protective, opposing, effects of calcium on *Hp*-induced gastritis in Mongolian gerbils. The mechanisms involved remain to be clarified. Interestingly, however, calcium may exert inhibitory effects on urease extraction from *Hp*. *Hp* urease is important for facilitating colonization of *Hp* and is correlated with stomach mucosal injury, including gastritis (22-24). Pérez-Pérez *et al*. showed that calcium chloride has little effect on *Hp* urease activity itself, but reduces extraction of urease from *Hp* cells (25). We have reported that urease inhibitors, acetohydroxamic acid and flurofamide, can eradicate *Hp* in Mongolian gerbils (26). These reports allow us to speculate that higher hydroxyapatite- or calcium carbonate-containing diets may eradicate *Hp* in Mongolian gerbils by the inhibition of *Hp* urease extraction.

Daily average intake of calcium by Japanese people from various foods, including fish bone and shrimp shell, is reported to be almost 500 mg per person (27). Thus, the doses of hydroxyapatite and calcium carbonate used in the present study are very much higher than the expected human exposure levels. However, humans continually consume various kinds of foods that may enhance *Hp*-induced gastritis. It is probable that calcium compounds and other dietary factors would have additional or synergistic enhancing effects on *Hp*-induced gastritis. Of note, it is reported that the content of hydroxyapatite-type calcium is around 36% in fish bone (28). This may also be true in the case of the content of calcium carbonate in prawn shell (29). Differences in enhancing effects of *Hp*-induced gastritis among the groups fed diets with hydroxyapatite, calcium carbonate, and calcium hydrogenphosphate dihydrate remain to be elucidated. Moreover, different effects of fishmeal treatment, fish bone treatment and direct calcium treatment on gastric mucosa should be taken into consideration because digestive processes should differ. From the incidence of hemorrhage in each group, direct calcium treatment at doses of 0.88 and 1.75% seem to induce more severe changes than 2% cod bone treatment or treatment with 4.5% 'other parts' diet. These data suggest that calcium itself could be the factor directly affecting functions related to *Hp*-induced gastritis.

The present experimental model may clarify the mechanism of development of peptic ulcer or acute mucosal lesions. This model does not represent chronic inflammation status that usually observed around human gastric cancer tissue because the experimental period is too short to induce chronic inflammation. However, in the *Hp*-infected Mongolian gerbil model with a long experimental period after carcinogen treatment, gastric cancer can be induced with similar pathological changes in humans. Our data may provide basic information for further experiments elucidating the mechanisms of gastric cancer induction.

Since the incidence of gastritis and gastric cancer is high all over the world, it is very important to clarify the effect of calcium on gastritis and to elucidate through further research the detailed mechanisms that enhance gastritis.

Acknowledgements

Authors thank Dr Takayuki Matsumoto, Dr Norihiko Kouyama, Dr Tomoko Mizote, Dr Hideyuki Shibata, Dr Toshihiko Kawamori and Dr Takeji Takamura for their valuable advice and help. We also thank Mr Masanobu Takiguchi for his technical assistance.

References

1 Nomura A: Stomach. *In*: Cancer Epidemiology and Prevention. Schottenfield D and Fraumeni J Jr. (eds.). Philadelphia, WB Saunders, pp. 624-637, 1982.
2 Ernst PB, Peura DA and Crowe SE: The translation of *Helicobacter pylori* basic research to patient care. Gastroenterol *130(1)*: 188-206, 2006.
3 Marshall BJ and Warren JR: Unidentified curved bacilli in the stomach of patients with gastritis and peptic ulceration. Lancet *1(8390)*: 1311-1315, 1984.
4 Parsonnet J, Friedman GD, Vandersteen DP, Vogelman JH, Orentreich N and Sibley RK: *Helicobacter pylori* infection and the risk of gastric carcinoma. N Engl J Med *325(16)*: 1127-1131, 1991.
5 Uemura N, Okamoto S, Yamamoto S, Matsumura N, Yamaguchi S, Yamakido M, Taniyama K, Sasaki N and Schlemper RJ: *Helicobacter pylori* infection and the development of gastric cancer. N Engl J Med *345(11)*: 784-789, 2001.
6 Hirayama F, Takagi S, Yokoyama Y, Iwao E and Ikeda Y: Establishment of gastric *Helicobacter pylori* infection in Mongolian gerbils. J Gastroenterol *31(9)*: 24-28, 1996.
7 Hirayama F, Takagi S, Kusuhara H, Iwao E, Yokoyama Y and Ikeda Y: Induction of gastric ulcer and intestinal metaplasia in Mongolian gerbils infected with *Helicobacter pylori*. J Gastroenterol *31(5)*: 755-757, 1996.
8 Shimizu N, Inada K, Nakanishi H, Tsukamoto T, Ikehara Y, Kaminishi M, Kuramoto S, Sugiyama A, Katsuyama T and Tatematsu M: *Helicobacter pylori* infection enhances glandular stomach carcinogenesis in Mongolian gerbils treated with chemical carcinogens. Carcinogenesis *20(4)*: 669-676, 1999.
9 Sugiyama A, Maruta F, Ikeno T, Ishida K, Kawasaki S, Katsuyama T, Shimizu N and Tatematsu M: *Helicobacter pylori* infection enhances *N*-methyl-*N*-nitrosourea-induced stomach carcinogenesis in the Mongolian gerbil. Cancer Res *58(10)*: 2067-2069, 1998.
10 Tokieda M, Honda S, Fujioka T and Nasu M: Effect of *Helicobacter pylori* infection on the *N*-methyl-*N*'-nitro-*N*-nitrosoguanidine-induced gastric carcinogenesis in mongolian gerbils. Carcinogenesis *20(7)*: 1261-1266, 1999.

11 Kato S, Tsukamoto T, Mizoshita T, Tanaka H, Kumagai T, Ota H, Katsuyama T, Asaka M and Tatematsu M: High salt diets dose-dependently promote gastric chemical carcinogenesis in *Helicobacter pylori*-infected Mongolian gerbils associated with a shift in mucin production from glandular to surface mucous cells. Int J Cancer *119(7)*: 1558-1566, 2006.

12 Matsubara S, Takasu S, Tsukamoto T, Mutoh M, Masuda S, Sugimura T, Wakabayashi K and Totsuka Y: Induction of glandular stomach cancers in *Helicobacter pylori*-infected Mongolian gerbils by 1-nitrosoindole-3-acetonitrile. Int J Cancer *130(2)*: 259-266, 2012.

13 Tanigawa T, Kawamori T, Iimuro M, Ohta T, Higuchi K, Arakawa T, Sugimura T and Wakabayashi K: Marked enhancement by fish meal of *Helicobacter pylori*-induced gastritis in Mongolian gerbils. Jpn J Cancer Res *91(8)*: 769-773, 2000.

14 Blaser MJ: Hypothesis: The changing relationships of *Helicobacter pylori* and humans: Implications for health and disease. J Infect Dis *181(2)*: 805-806, 2000.

15 International Agency for Research on Cancer: Schistosomes, Liver Flukes and *Helicobacter pylori*. *In*: IARC Monogr Eval Carcinog Risks Hum 61. Lyon, IARC, pp. 177-240, 1994.

16 Kirchhoff P and Geibel JP: Role of calcium and other trace elements in the gastrointestinal physiology. World J Gastroenterol *12(20)*: 3229-3236, 2006.

17 Furihata C, Yamakoshi A, Takezawa R and Matsushima T: Various sodium salts, potassium salts, a calcium salt and an ammonium salt induced ornithine decarboxylase and stimulated DNA synthesis in rat stomach mucosa. Jpn J Cancer Res *80(5)*: 424-429, 1989.

18 Tatsuta M, Iishi H, Baba M, Nakaizumi A, Uehara H and Taniguchi H: Effect of calcium channel blockers on gastric carcinogenesis and caerulein enhancement of gastric carcinogenesis induced by *N*-methyl-*N*'-nitro-*N*-nitrosoguanidine in Wistar rats. Cancer Res *50(7)*: 2095-2098, 1990.

19 Ghanayem BI, Matthews HB and Maronpot RR: Calcium channel blockers protect against ethanol- and indomethacin-induced gastric lesions in rats. Gastroenterology *92(1)*: 106-111, 1987.

20 You WC, Blot WJ, Chang YS, Ershow AG, Yang ZT, An Q, Henderson B, Xu GW, Fraumeni JF Jr. and Wang TG: Diet and high risk of stomach cancer in Shandong, China. Cancer Res *48(12)*: 3518-3523, 1988.

21 Furihata C, Sudo K and Matsushima T: Calcium chloride inhibits stimulation of replicative DNA synthesis by sodium chloride in the pyloric mucosa of rat stomach. Carcinogenesis *10(11)*: 2135-2137, 1989.

22 Eaton KA, Brooks CL, Morgan DR and Krakowka S: Essential role of urease in pathogenesis of gastritis induced by *Helicobacter pylori* in gnotobiotic piglets. Infect Immun *59(7)*: 2470-2475, 1991.

23 Chen XG, Correa P, Offerhaus J, Rodriguez E, Janney F, Hoffmann E, Fox J, Hunter F and Diavolitsis S: Ultrastructure of the gastric mucosa harboring *Campylobacter*-like organisms. Am J Clin Pathol *86(5)*: 575-582, 1986.

24 Hazell SL, Lee A, Hazell SL and Lee A: *Campylobacter pyloridis*, urease, hydrogen ion back diffusion, and gastric ulcers. Lancet *2(8497)*: 15-17, 1986.

25 Pérez-Pérez GI, Gower CB and Blaser MJ: Effects of cations on *Helicobacter pylori* urease activity, release, and stability. Infect Immun *62(1)*: 299-302, 1994.

26 Ohta T, Shibata H, Kawamori T, Iimuro M, Sugimura T and Wakabayashi K: Marked reduction of *Helicobacter pylori*-induced gastritis by urease inhibitors, acetohydroxamic acid and flurofamide, in Mongolian gerbils. Biochem Biophys Res Commun *285(3)*: 728-733, 2001.

27 National Health and Nutrition Survey 2009. *In*: Ministry of Health, Labour and Welfare Japan, 2009. Available at: http://www.mhlw.go.jp/bunya/kenkou/eiyou/dl/h21-houkoku-01.pdf

28 Hamada M, Nagai T, Kai N, Tanoue Y, Mae H, Hashimoto M, Miyoshi K, Kumagai H and Saeki K: Inorganic constituents of bone of fish. Fisheries Sci *61(3)*: 517-520,1995.

29 Xu Y, Gallert C and Winter J: Chitin purification from shrimp wastes by microbial deproteination and decalcification. Appl Microbiol Biotechnol *79*: 687-697, 2008.

Received July 8, 2013
Revised July 26, 2013
Accepted July 29, 2013

Ann Nucl Med (2013) 27:640–647
DOI 10.1007/s12149-013-0729-1

ORIGINAL ARTICLE

SPECT/CT of lung nodules using ^{111}In-DOTA-c(RGDfK) in a mouse lung carcinogenesis model

Takuya Hayakawa · Michihiro Mutoh · Toshio Imai · Koji Tsuta · Akinori Yanaka · Hirofumi Fujii · Mitsuyoshi Yoshimoto

Received: 16 October 2012 / Accepted: 10 April 2013 / Published online: 23 April 2013

Abstract
Objective Lung cancer is one of the leading causes of cancer-related deaths worldwide, including Japan. Although computed tomography (CT) can detect small lung lesions such as those appearing as ground glass opacity, it cannot differentiate between malignant and non-malignant lesions. Previously, we have shown that single photon emission computed tomography (SPECT) imaging using ^{111}In-1,4,7,10-tetraazacyclododecane-*N*,*N*′,*N*″,*N*‴-tetraacetic acid-cyclo-(Arg-Gly-Asp-D-Phe-Lys) (DOTA-c(RGDfK)), an imaging probe of $\alpha_v\beta_3$ integrin, is useful for the early detection of pancreatic cancer in a hamster pancreatic carcinogenesis model. In this study, we aimed to assess the usefulness of SPECT/CT with ^{111}In-DOTA-c(RGDfK) for the evaluation of the malignancy of lung cancer.
Methods Lung tumors were induced by a single intraperitoneal injection (250 mg/kg) of urethane in male A/J mice. Twenty-six weeks after the urethane treatment, SPECT was performed an hour after injection of ^{111}In-DOTA-c(RGDfK). Following this, the radioactivity ratios of tumor to normal lung tissue were measured by autoradiography (ARG) in the excised lung samples. We also examined the expression of $\alpha_v\beta_3$ integrin in mouse and human lung samples.
Results Urethane treatment induced 5 hyperplasias, 41 adenomas and 12 adenocarcinomas in the lungs of 8 A/J mice. SPECT with ^{111}In-DOTA-c(RGDfK) could clearly visualize lung nodules, though we failed to detect small lung nodules like adenoma and hyperplasias (adenocarcinoma: 66.7 %, adenoma: 33.6 %, hyperplasia: 0.0 %). ARG analysis revealed significant uptake of ^{111}In-DOTA-c(RGDfK) in all the lesions. Moreover, tumor to normal lung tissue ratios increased along with the progression of carcinogenesis. Histopathological examination using human lung tissue samples revealed clear up-regulation of $\alpha_v\beta_3$ integrin in well-differentiated adenocarcinoma (Noguchi type B and C) rather than atypical adenomatous hyperplasia.
Conclusion Although there are some limitations in evaluating the malignancy of small lung tumors using ^{111}In-DOTA-c(RGDfK), SPECT with ^{111}In-DOTA-c(RGDfK) might be a useful non-invasive imaging approach for evaluating the characteristics of lung tumors in mice, thus showing potential for use in humans.

Keywords ^{111}In-DOTA-c(RGDfK) · SPECT · Carcinogenesis · Lung cancer

T. Hayakawa · M. Mutoh
Division of Cancer Prevention Research, National Cancer Center Research Institute, 5-1-1 Chuo-ku, Tokyo 104-0045, Japan

T. Hayakawa · A. Yanaka
Faculty of Pharmaceutical Sciences, Tokyo University of Science, 2641 Yamazaki, Noda, Chiba 278-8510, Japan

T. Imai
Central Animal Division, National Cancer Center Research Institute, 5-1-1 Chuo-ku, Tokyo 104-0045, Japan

K. Tsuta
Division of Pathology and Clinical Laboratory, National Cancer Center Hospital, 5-1-1 Chuo-ku, Tokyo 104-0045, Japan

H. Fujii · M. Yoshimoto
Functional Imaging Division, National Cancer Center Hospital East, 6-5-1 Kashiwanoha, Kashiwa, Chiba 277-8577, Japan

M. Yoshimoto (✉)
Division of Cancer Development System, National Cancer Center Research Institute, 5-1-1 Tsukiji, Chuo-ku, Tokyo 104-0045, Japan
e-mail: miyoshim@ncc.go.jp

algorithm on dedicated software (Invivoscope; Bioscan, Inc., Washington, DC, USA) and Mediso InterViewXP (Mediso, Budapest, Hungary). SPECT and CT images were automatically superimposed by Invivoscope. The accuracy of superimposition was calibrated at regular intervals using phantoms. A researcher experienced in the evaluation of small animal SPECT/CT images visually judged pulmonary uptake.

Autoradiography with ^{111}In-DOTA-c(RGDfK) in the mouse lung carcinogenesis model

After SPECT/CT imaging, the lungs were excised and macroscopically surveyed to detect lung tumor lesions. Samples were then embedded in Cryo Mount II (Muto Pure Chemicals Co., Ltd., Tokyo, Japan) and frozen in liquid nitrogen. Frozen sections were mounted on glass slides after being cut with a cryostat into 20-μm thick sections for autoradiography (ARG) and 10-μm thick sections for histological analysis. The glass slides were then placed on an imaging plate (BAS-MS 2040; Fuji film Co., Ltd., Tokyo, Japan). Radioactivity was detected by scanning with a bioimaging analyzer (FLA-7000, Fuji film Co., Ltd., Tokyo, Japan). Based on the microscopic observation of hematoxylin and eosin (H&E) stained sections, regions of interest were placed on both tumor and normal lung regions. Image Quant software (Multi gauge, Fuji film Co., Ltd., Tokyo, Japan) was used to quantify the intensity of radioactivity.

Human lung tissue microarray (TMA)

The expression of $\alpha_v\beta_3$ integrin in various types of human lung lesions was tested using TMA. A total of 48 tissue samples were embedded in TMA sections, including bronchial tubes, normal lung tissue, adenocarcinoma (poorly, moderately, and well differentiated), squamous cell carcinoma, large cell neuroendocrine carcinoma, and mesothelioma. The study protocol was approved by the institutional review board of the NCC, Tokyo, Japan.

Human lung tissue samples

A total of 34 lung tissue samples were obtained from patients who underwent lobectomies at the National Cancer Center (NCC) Hospital from 2006 to 2008. The paraffin-embedded sample stocks were immunohistochemically stained for $\alpha_v\beta_3$ integrin. The samples included atypical adenomatous hyperplasia (AAH, $n = 16$), localized bronchioloalveolar carcinoma with alveolar collapse (Noguchi type B, $n = 11$), and localized bronchioloalveolar carcinoma with foci of active fibroblastic proliferation (Noguchi type C, $n = 10$), which could be classified as GGOs on clinical CT images. The study protocol was approved by the institutional review board of the NCC, Tokyo, Japan.

Immunohistochemistry for $\alpha_v\beta_3$ integrin

The excised mice and human lung sections were used for immunohistochemical examination using the avidin–biotin complex immunoperoxidase technique. Sections were incubated with anti-$\alpha_v\beta_3$ integrin (clone LM609; Millipore, Billerica, MA, USA) overnight at 4 °C. Sections were incubated with biotinylated anti-mouse IgG (Dako Cytomation, Glostrup, Denmark), followed by reaction with streptavidin–biotin horseradish peroxidase (HRP) complex (Strept ABComplex/HRP; Dako Cytomation). HRP was detected by 3,3′-diaminobenzidine (Phoenix Biotechnologies, Huntsville, AL, USA) substrate. All sections were counterstained with hematoxylin.

Evaluation of staining intensity

Sections were evaluated randomly without knowledge of patient history. Each specimen wherein more than 10 % of the cancer cells reacted positively for an antibody were recorded as positive. The sections were classified according to staining intensity as negative (total absence of staining), 1+ (weak staining), 2+ (moderate staining), or 3+ (strong staining).

Statistical analysis

Statistical analysis was performed using JMP IN version 5 statistical software (SAS Institute, Cary, NC, USA). Mann–Whitney test was employed to numerical data that did not show a normal distribution (comparison of T/N ratio). χ^2 tests were applied to compare the difference in the detection rate using SPECT in different tumor stage. Values are reported as mean ± SD. A two-tailed p value of <0.05 was considered statistically significant.

Results

SPECT with ^{111}In-DOTA-c(RGDfK) in the urethane-treated mice

In total, 58 lung lesions were macroscopically found in the 8 urethane-treated mice. Of the 58 lesions, 12 were adenocarcinomas (average size, 1.87 ± 0.58 mm), 41 were adenomas (average size, 1.45 ± 0.31 mm), and 5 were hyperplasias (average size, 1.34 ± 0.42 mm). As shown in Table 1, SPECT with ^{111}In-DOTA-c(RGDfK) detected 8 adenocarcinomas (66.7 %), 15 adenomas (36.6 %), and 0 hyperplasias (0.0 %). These detection rates were

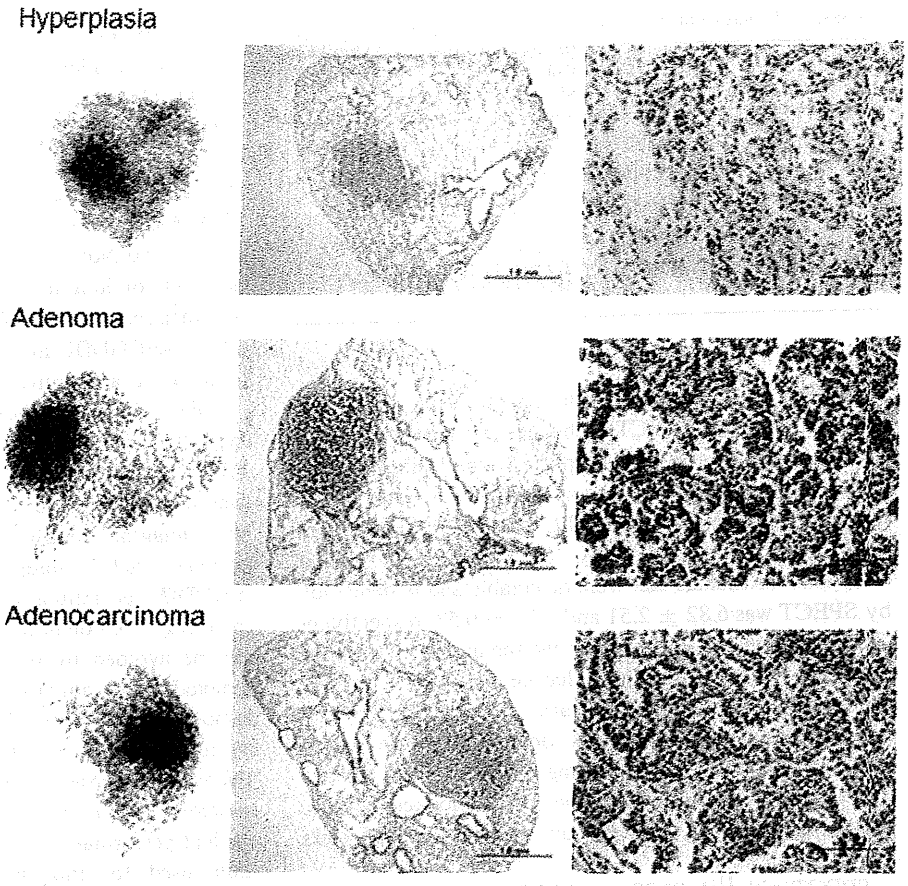

Fig. 2 Ex vivo autoradiography and H&E staining of representative lung sections. Strong hot spots were found in the right upper lobes by ARG (*left lane*). H&E staining of lung sections (*middle lane*) and high magnification of lung lesions (*right lane*)

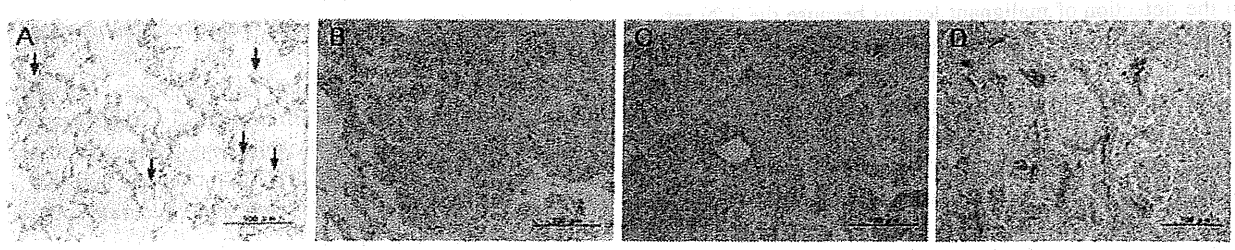

Fig. 3 $\alpha_v\beta_3$ integrin expression in the lung lesions of A/J mice. **a** Normal lung tissue. Type II pneumocytes expressing negligible levels of $\alpha_v\beta_3$ integrin (*arrow*). **b** Hyperplasia, **c** adenoma, and **d** adenocarcinoma

of $\alpha_v\beta_3$ integrin was observed in type II pneumocyte and Clara cells (Figs. 3a and 4c). Consistent with this observation, ^{111}In-DOTA-c(RGDfK) was accumulated in bronchial tubes of the A/J mice (Fig. 4a).

Expression of $\alpha_v\beta_3$ integrin in various types of human lung tumors

Expression of $\alpha_v\beta_3$ integrin was evaluated using TMA including several tissue types such as adenocarcinoma, squamous cell carcinoma, large cell neuroendocrine carcinoma, and mesothelioma. Among them, strong and extensive immunoreactivity for $\alpha_v\beta_3$ integrin was found in differentiated tubular adenocarcinoma.

We further examined staining intensity of $\alpha_v\beta_3$ integrin in AAH, Noguchi type B and Noguchi type C lesions (Fig. 5), and the incidence of positive cases is summarized in Table 2. The incidence of $\alpha_v\beta_3$ integrin-positivity was high for Noguchi type B (91 %) and Noguchi type C (90 %). In contrast, relatively lower expression (63 %) was observed in AAH lesions.

Staining intensity correlated with tumor aggressiveness. The incidence of strong positivity (+++) among the AAH, Noguchi type B, and Noguchi type C lesions was 6.3, 27.3,

Table 2 Incidence of $\alpha_v\beta_3$ integrin expression in human lung lesions

$\alpha_v\beta_3$ Intensity	AAH (%)	Noguchi type B (%)	Noguchi type C (%)
−	6/16 (37.5)	1/11 (9.1)	1/10 (10.0)
+	3/16 (18.8)	1/11 (9.1)	1/10 (10.0)
++	6/16 (37.5)	6/11 (54.5)	3/10 (30.0)
+++	1/16 (6.3)	3/11 (27.3)	5/10 (50.0)
Total positive lesions	10/16 (62.5)	10/11 (90.9)	9/10 (90)

Therefore, a low detection rate may be explained by the limitations of the SPECT technique itself with regard to small lesion size and/or low uptake in the lesions. In fact, the average size of the adenocarcinomas that were detectable and undetectable by SPECT was 2.09 ± 0.59 and 1.43 ± 0.17 mm, respectively. The average T/N ratio of the adenocarcinomas that were detectable and undetectable by SPECT was 6.82 ± 2.51 and 4.27 ± 0.53, respectively. Therefore, the size of the tumor and the uptake of tracer by the tumor have significant influence on SPECT images. The low detection rate may also be explained by the deterioration of SPECT images. Because of movement of the heart and the thoracic diaphragm, lesions in the hilus of the lung or at the periphery may be overlooked because cardiac motion may prevent the visualization of clear images.

SPECT with ^{111}In-DOTA-c(RGDfK) seems to be useful in the detection of malignant lesions because the T/N ratio of adenocarcinoma is significantly greater than that of hyperplasia ($p < 0.05$). Moreover, in accordance with the increase of the T/N ratio, the detection rate by SPECT was highest in adenocarcinomas. We could not show the relationship between the uptake of ^{111}In-DOTA-c(RGDfK) and the $\alpha_v\beta_3$ integrin expression level in this study because the condition of the tissue samples used in the present SPECT study was poor for the immunohistochemical semi-quantitative analysis. However, it has already been reported that the accumulation level of RGD peptide probe correlates with the expression level of $\alpha_v\beta_3$ integrin [16]. Thus, it is thought that the difference of accumulation level of ^{111}In-DOTA-c(RGDfK) between adenocarcinoma, adenoma, and hyperplasia in our present study is also reflecting the expression level of $\alpha_v\beta_3$ integrin.

The role of the $\alpha_v\beta_3$ integrin in lung cancer is unclear. However, the $\alpha_v\beta_3$ expression in breast cancer, pancreatic cancer, and prostate cancer contributes to tumor progression and metastasis [17–19]. High uptake of ^{111}In-DOTA-c(RGDfK) by lung cancer lesions might estimate metastatic potential to spread to the brain and bones.

We recently reported that ^{111}In-DOTA-c(RGDfK) is superior to 2-deoxy-2-[^{18}F]fluoro-D-glucose in the differentiation of inflammatory lesions [13]. It is highly effective in identifying malignant lesions that appear as GGOs. During histopathological examination of human lung tissue samples, we observed a high incidence and the strong expression of $\alpha_v\beta_3$ integrin in Noguchi type B and Noguchi type C lesions. These results suggested that ^{111}In-DOTA-c(RGDfK) would preferentially identify Noguchi type B and Noguchi type C. At present, there are no other methods of long-term follow-up for the determination of the malignancy of GGOs. SPECT/CT imaging with ^{111}In-DOTA-c(RGDfK) may help in determining whether biopsy to arrive at a definitive diagnosis should be performed.

Our histopathological examination also revealed that type II pneumocytes express low levels of $\alpha_v\beta_3$ integrin. Although $\alpha_v\beta_3$ integrin expression in type II pneumocytes was negligible in our study, it did not appear to interfere with imaging contrast. We also found that Clara cells express $\alpha_v\beta_3$ integrin. Furthermore, ^{111}In-DOTA-c(RGDfK) accumulated in the bronchial tubes of the A/J mice (Fig. 1). Potentially, this type of false positive finding can be avoided by procuring CT images because reconstructed three-dimensional images easily differentiate tumors (globular) and bronchial tubes (tube structure) in the lungs, even though both have similar X-ray absorption. Therefore, combined SPECT/CT has the potential to overcome the limitations of SPECT alone. Because the clinical performance of CT scanners is better than that of units used for imaging small animals with regard to acquisition time, tube voltage, and current × time product (mAs), identification of the lung structure would be easier in clinical practice.

Furthermore, in our animal experiments, breathing motion affected the degradation of SPECT images because of the long acquisition time. Respiratory-gating systems are now available in clinical SPECT/CT scanners, and this is aiding in the procurement of much more accurate images. Therefore, when CT and SPECT are combined, clearer images can be obtained in clinical practice.

Recently, clinical examinations using ^{99m}Tc-3PRGD for imaging of lung cancer have reported that ^{99m}Tc-3PRGD imaging has sensitivity for the detection of lung malignancies, though the specificity is low [20, 21]. Our study using a carcinogenesis animal model and human tissue samples has provided helpful information that can aid in the diagnosis of lung tumors using radiolabeled RGD.

Conclusion

The present study demonstrated that there are some limitation in detecting mouse lung tumors by SPECT/CT imaging using ^{111}In-DOTA-c(RGDfK), but ^{111}In-DOTA-c(RGDfK) has a possibility to evaluate the malignancy of

Cancer Science
The official journal of the Japanese Cancer Association

A^y allele promotes azoxymethane-induced colorectal carcinogenesis by macrophage migration in hyperlipidemic/diabetic KK mice

Kumiko Ito,[1,2] Rikako Ishigamori,[1] Michihiro Mutoh,[1] Toshihiro Ohta,[2] Toshio Imai[3] and Mami Takahashi[3,4]

[1]Division of Cancer Prevention Research, National Cancer Center Research Institute, Tokyo; [2]School of Life Sciences, Tokyo University of Pharmacy and Life Sciences, Tokyo; [3]Central Animal Division, National Cancer Center Research Institute, Tokyo, Japan

(Received January 4, 2013/Revised March 18, 2013/Accepted March 19, 2013/Accepted manuscript online April 2, 2013/Article first published online May 24, 2013)

The incidence of colorectal cancer has been increasing and is associated with obesity and diabetes. We have found that type 2 diabetes model KK-A^y/TaJcl (KK-A^y) mice develop tumors within a short period after treatment with azoxymethane (AOM). However, factors that contribute to the promotion of carcinogenesis have not been clarified. Therefore, we looked at the genetic background of KK-A^y, including two genetic characteristics of KK/TaJcl (KK) mice and C57BL/6J-Ham-A^y/+ (A^y) mice, compared with other non-obese and non-diabetic mouse strains C57BL/6J and ICR, and induced colorectal premalignant lesions, aberrant crypt foci (ACF), and tumors using AOM (150 μg/mouse/week for 4 weeks and 200 μg/mouse/week for 6 weeks, respectively). The mice with a diabetes feature, KK-A^y and KK, developed significantly more ACF, 67 and 61 per mouse, respectively, whereas ICR, A^y, and C57BL/6J mice developed 42, 24, and 18 ACF/mouse, respectively, at 17 weeks of age. Serum insulin and triglyceride levels in KK-A^y and KK mice were quite high compared with other non-diabetic mouse strains. Interestingly, KK-A^y mice developed more colorectal tumors (2.7 ± 2.3 tumor/mouse) than KK mice (1.2 ± 1.1 tumor/mouse) at 25 weeks of age, in spite of similar diabetic conditions. The colon cancers that developed in both KK-A^y and KK mice showed similar activation of β-catenin signaling. However, mRNA levels of inflammatory factors related to the activation of macrophages were significantly higher in colorectal cancer of KK-A^y mice than in KK. These data indicate that factors such as insulin resistance and dyslipidemia observed in obese and diabetic patients could be involved in susceptibility to colorectal carcinogenesis. In addition, increase of tumor-associated macrophages may play important roles in the stages of promotion of colorectal cancer. (*Cancer Sci* 2013; 104: 835–843)

Excessive accumulation of visceral adipose tissue can induce many disorders, such as type 2 diabetes mellitus (elevated fasting glucose, insulin, and insulin-like growth factor levels), and dyslipidemia (elevated triglyceride or low high-density lipoprotein cholesterol levels). Obesity is common in Western countries, and is currently increasing almost ubiquitously across the globe. Recently, obesity has attracted much interest as a risk factor for colorectal cancer. The World Cancer Research Fund and American Institute for Cancer Research have evaluated causal relationships between accumulation of visceral adipose tissue and cancer, and concluded "confident evidence" for colorectal cancers.[1] In males in Japan, an overweight condition and obesity (body mass index ≥ 25) are reported to be associated with colorectal cancer.[2,3]

We have reported that obese KK-A^y mice are highly susceptible to induction of colorectal premalignant lesions, ACF, and to development of colorectal cancers by AOM treatment.[4] The KK-A^y mice feature severe hyperinsulinemia, severe hypertriglyceridemia, excessive abdominal obesity, and resultant elevation of serum adipocytokines, such as IL-6, leptin, and Pai-1 compared with values for lean C57BL/6J mice. Such a consequent abnormality is suggested to be involved in the promotion of colorectal carcinogenesis, and is partly considered as a factor for high cancer susceptibility.

The KK-A^y mice were established by cross-mating KK mice, a type 2 diabetes mellitus model, with A^y mice,[5,6] which carry the *Agouti yellow* (A^y) gene and feature severe hyperphagia, hyperinsulinemia, and dyslipidemia. Non-diabetic or non-obese mice could be set as control, e.g., young A^y mice or C57BL/6J-Ham-+/+ (+/+) mice. In addition to this, the body weight of ICR mice is almost the same as KK-A^y mice at a young age, and they are also susceptible to induction of colorectal carcinogenesis by AOM treatment. The strains and features that could be the most susceptible to induction of colorectal carcinogenesis by AOM treatment have not been clarified. Thus, we aimed to investigate and find the features and molecules involved in obesity-associated cancer by comparing mouse strains KK-A^y, KK, A^y, +/+, C57BL, and ICR. In the present study, we showed colorectal ACF development was strongly affected by diabetic conditions, and additional features of inflammation derived from agouti gene overexpression may lead to further promotion of cancer development.

Materials and Methods

Animals. Female 5-week-old KK-A^y, KK, C57BL, and ICR mice were purchased from CLEA Japan (Tokyo, Japan), and A^y and +/+ mice were purchased from SLC Japan (Shizuoka, Japan). All animals were acclimated to laboratory conditions for 1 week. Three to four mice were housed per plastic cage with sterilized softwood chips as bedding in a barrier-sustained animal room at 22 ± 1°C and 55% humidity on a 12:12 h light:dark cycle, and fed AIN-76A powdered basal diet (CLEA Japan). Food and water were available *ad libitum*. The animals were observed daily for clinical signs, including anal bleeding and mortality. Body weights and food and water consumption were measured weekly. The experiments were carried out according to the Guidelines for Animal Experiments in the National Cancer Center (National Cancer Center, Tokyo, Japan) and were approved by the Institutional Ethics Review Committee for Animal Experimentation in the National Cancer Center.

Azoxymethane-induced colorectal ACF development. For the induction of ACF by AOM (Nard Institute, Amagasaki, Japan), 6-week-old female KK-A^y (n = 13), KK (n = 13), A^y (n = 12), +/+ (n = 12), C57BL/6J (n = 13), and ICR (n = 13) mice

[4]To whom correspondence should be addressed.
E-mail: mtakahas@ncc.go.jp

doi: 10.1111/cas.12162

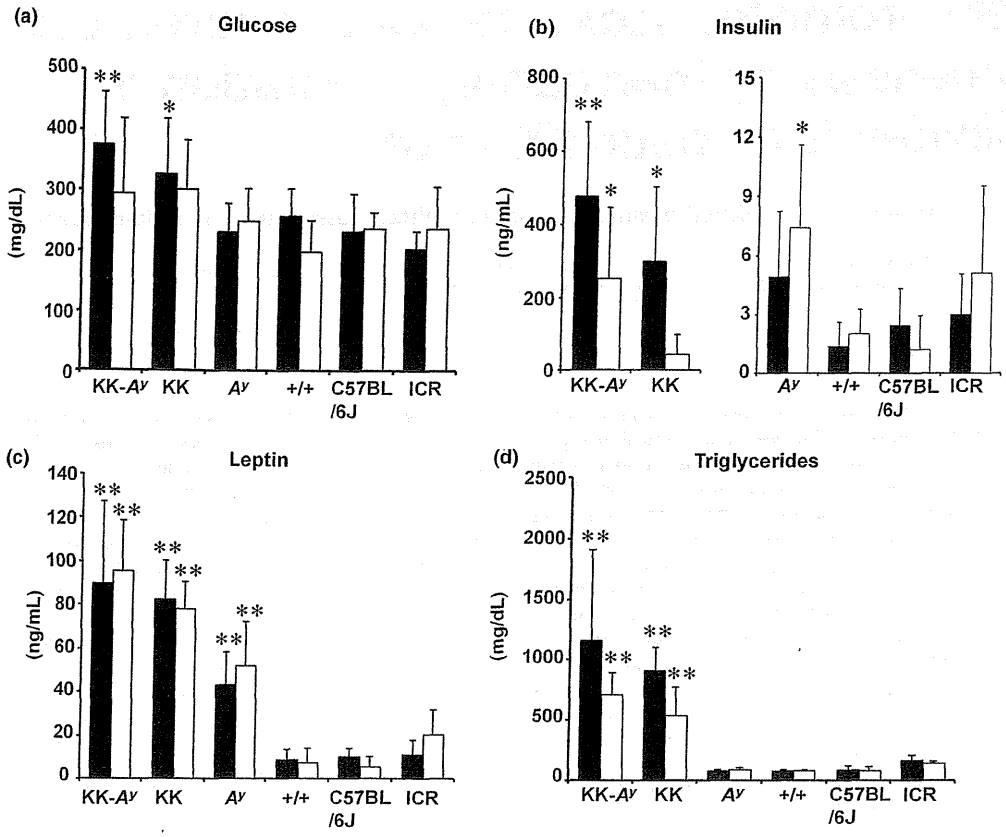

Fig. 2. Parameters for diabetes in KK-A^y/TaJcl (KK-A^y), KK/TaJcl (KK), and ICR mice treated with or without azoxymethane (AOM). The data of the group treated with AOM six times are shown in an open box, and without AOM are shown in a closed box. Parameters for diabetes, such as blood glucose (a), serum insulin levels (b), serum leptin levels (c), and serum triglyceride levels (d) are shown in the indicated mice strain. Data are mean ± SD. *P < 0.05, **P < 0.01 *vs* ICR mice. +/+, C57BL/6J-Ham-+/+; A^y, C57BL/6J-Ham-A^y/+.

Table 1. Development of colorectal aberrant crypt foci (ACF) in six strains of mice treated with azoxymethane

Strain of mice	No. of mice with ACF	No. of ACF/colorectum				
		Proximal	Middle	Distal	Rectum	Total
KK-A^y	13/13	0.3 ± 0.5	16.7 ± 9.0**	36.0 ± 24.0**	13.7 ± 7.1*	66.7 ± 35.4**
KK	13/13	0.8 ± 1.0*	14.2 ± 6.2**	31.4 ± 8.2**	14.6 ± 7.3**	61.0 ± 17.4**
A^y	12/12	0.0 ± 0.0	1.9 ± 2.1	15.7 ± 6.7*	6.1 ± 2.3	23.7 ± 8.6
+/+	12/12	0.0 ± 0.0	3.4 ± 1.9	12.3 ± 4.6	6.6 ± 4.2	22.3 ± 6.9
C57BL/6J	13/13	0.1 ± 0.3	1.6 ± 2.3	9.3 ± 3.0	7.0 ± 2.2	18.0 ± 5.4
ICR	13/13	0.1 ± 0.3	7.7 ± 4.4*	27.2 ± 12.0**	6.9 ± 4.8	41.9 ± 18.7**

Data are expressed as mean ± SD. *P < 0.05, **P < 0.01 versus C57BL/6J-Ham-+/+ (+/+). A^y, C57BL/6J-Ham-A^y/+; KK, KK/TaJcl; KK-A^y, KK-A^y/TaJcl.

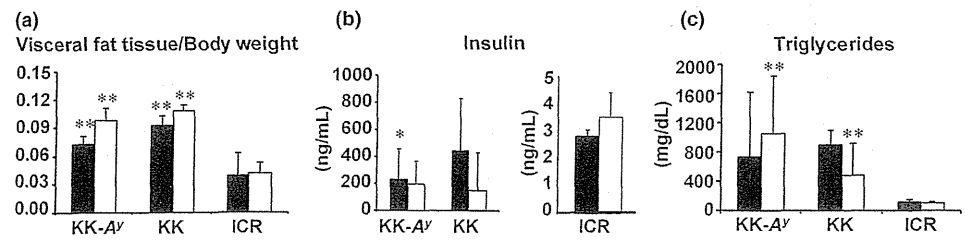

Fig. 3. Parameters for diabetes in KK-A^y/TaJcl (KK-A^y), KK/TaJcl (KK), and ICR mice treated with or without azoxymethane (AOM). The data of the group treated with AOM six times are shown in an open box, and without AOM are shown in a closed box. Parameters for diabetes, such as visceral fat weight/body weight (a), serum insulin levels (b), and serum triglyceride levels (c) are shown in the indicated mice strain. Data are mean ± SD. *P < 0.05, ** P< 0.01 *vs* ICR mice.

and C57BL/6J mice at 6 weeks of age (18–16 g), but markedly higher than those mice at the end of the experiment. In the ACF experiment with 4-times AOM treatment (ACF experiment), the final mean body weights at 17 weeks of age of KK-A^y, KK, ICR, A^y, +/+, and C57BL/6J mice with AOM treatment were 48.3 ± 4.7 g (mean ± SD), 44.8 ± 2.4, 40.6 ± 5.9, 30.8 ± 4.5, 20.4 ± 1.4, and 22.1 ± 1.3 g, respectively, and mean daily food intakes were 4.2 ± 1.1, 3.8 ± 0.3, 3.8 ± 0.3, 3.3 ± 0.6, 2.9 ± 0.1 and 2.9 ± 0.1 g/mouse/day, respectively. Thus, KK-A^y and A^y mice ate more than the respective control mouse strains. In the colorectal cancer experiment with 6-times AOM treatment (colorectal cancer experiment), the final mean body weights at 25 weeks of age of KK-A^y and KK mice with AOM treatment were significantly higher than those of ICR mice, being 54.2 ± 4.8, 46.9 ± 4.8, and 41.1 ± 5.9 g, respectively; furthermore, KK-A^y mice were significantly heavier than KK mice. Of note, weights of visceral fat in KK-A^y and KK mice were also significantly higher than those of ICR mice (Fig. 1b).

Diabetes status observed in KK-A^y and KK mice. Serum concentrations of glucose, insulin, leptin, and triglycerides at age 17 weeks were measured to evaluate characteristics of glucose metabolism between the strains (Fig. 2). Among the strains, KK-A^y and KK mice showed high serum glucose, insulin, and triglyceride levels, a feature of diabetes, in non-AOM-treated mice. Serum insulin and triglyceride levels in non-diabetic mice (A^y, +/+, C57BL/6J mice, and ICR) were all less than 15 ng/dL and 250 mg/dL, respectively. However, serum insulin levels in KK-A^y and KK mice were 478.3 ± 201.5 (mean ± SD) ($P < 0.01$ *vs* A^y) and 299.4 ± 201.6 ng/dL ($P < 0.01$ *vs* A^y), respectively. Serum triglyceride levels in KK-A^y and KK mice were 1158 ± 748 (mean ± SD) ($P < 0.01$ *vs* A^y) and 910 ± 191.0 mg/dL ($P < 0.01$ *vs* A^y), respectively. Serum leptin levels in A^y mice were also elevated compared to those of +/+ mice, but lower than those of KK-A^y and KK mice. Similar results were obtained in the mice treated with AOM.

Increased number of colorectal aberrant crypt foci in KK-A^y and KK mice. All KK-A^y, KK, A^y, +/+, C57BL/6J, and ICR mice developed ACF in the colon and rectum at 17 weeks with AOM treatment (Table 1). In spite of the treatment of all mice with AOM at the same dosage (150 μg/mouse [≈10 mg/kg], weekly for 4 weeks), induction of colorectal ACF was much greater in KK-A^y and KK mice compared to other non-diabetic mice, that is, A^y, +/+, C57BL/6J, and ICR mice. The numbers of total ACF per mouse in KK-A^y and KK mice were 66.7 ± 35.4 and 61.0 ± 17.4 (mean ± SD), which were almost three times higher than those in +/+ mice. Significantly higher numbers of colorectal ACF in KK-A^y and KK mice were observed in all portions of the colorectum compared with +/+ mice, but they were most abundant in the distal portion. The ICR mice were also susceptible to induction of ACF (41.9 ± 18.7/mouse), but the value was less than KK-A^y and KK mice. Saline-treated mice did not develop colorectal ACF.

Increased incidence, number, and size of colorectal tumors in KK-A^y mice. Serum concentrations of glucose, insulin, leptin, and triglycerides at the age of 25 weeks were similar to those at the age of 17 weeks. Serum insulin and triglyceride levels in KK-A^y, KK, and ICR mice at 25 weeks of age are shown in Figure 3.

As shown in Table 2, the incidence of colorectal tumors developed in the KK-A^y and KK mice by AOM treatment was 87% and 73%, respectively, the value in KK-A^y mice tending to be higher. No tumors were observed in ICR mice by 25 weeks of age. Incidences of colorectal tumors in A^y and +/+ mice were both 0 out of 3 at 30 weeks of age (0%), and 0 out of 15 (0%) and 3 out of 14 (20%) at 55 weeks of age, respectively, showing that A^y mice with a C57BL/6J background were not susceptible to colon carcinogenesis. Most colorectal tumors developed in KK-A^y and KK mice were distributed in the middle to distal portion (Fig. 4a–d). Most large tumors developed in KK-A^y mice were red-colored (Fig. 4a,b), and red blood cells were observed to be abundant in those tumors (Fig. 4f). Histopathological examination revealed most AOM-induced colorectal tumors to be adenocarcinomas (Fig. 4e–h). Table 2 also summarizes data on multiplicity (number of tumors/mouse). The average number of tumors in KK-A^y mice was more than twice that in KK mice ($P < 0.05$). The predominant histological types of carcinomas in KK-A^y mice were well-differentiated.

The number of large tumors (diameter ≥5 mm) was significantly higher in KK-A^y mice than in KK mice, and average tumor volume per mouse in KK-A^y mice was more than threefold that in KK mice (Fig. 5), suggesting tumor promotion due to *agouti* gene overexpression in KK-A^y mice.

Activation of macrophages involved in cancer promotion is suggested to be the difference between KK-A^y and KK mice. To evaluate the activation of β-catenin signaling in AOM-induced colorectal cancer in KK-A^y and KK mice, nuclear localization of β-catenin (active form of β-catenin) was examined by immunohistochemistry (Fig. 6). Nuclear localization of β-catenin was not observed in the tumor surrounding normal parts of colorectal mucosa. β-catenin was clearly activated only in cancerous parts of the colorectum.

Translocation of β-catenin to the nucleus, as shown in Figure 6(a,b), suggested transcriptional activation of β-catenin-responsive genes. Thus, we carried out semiquantitative RT-PCR to confirm the activation of β-catenin signaling pathways. Cyclooxygenase-2, cyclin D1, and Pai-1 mRNA, the β-catenin target genes, in the non-cancerous part and cancerous part of

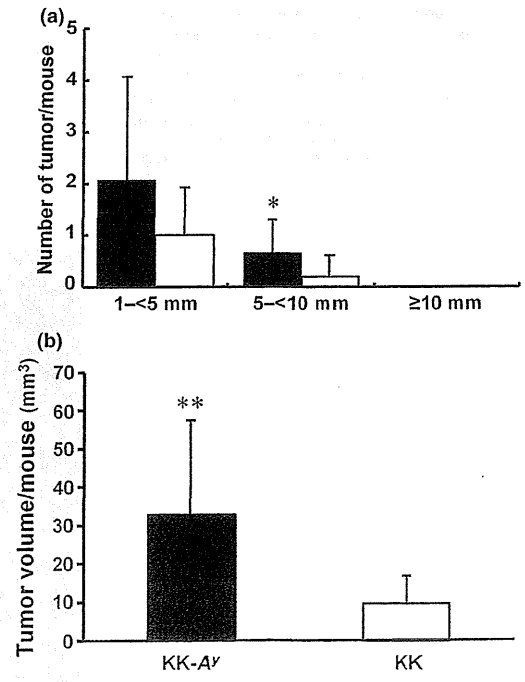

Fig. 5. Tumor size difference observed in azoxymethane-treated KK-A^y/TaJcl (KK-A^y) and KK/TaJcl (KK) mice at the age of 25 weeks. (a) Azoxymethane-developed tumors were divided into three groups by longitudinal diameter, 1–<5 mm, 5–<10 mm, and ≥10 mm. (b) Tumor volume was calculated using the formula, V = length × diameter (short) × diameter (long). ■, KK-A^y mice; □, KK mice. Data are mean ± SD. *$P < 0.05$, **$P < 0.01$ *vs* tumor volume of KK mice.

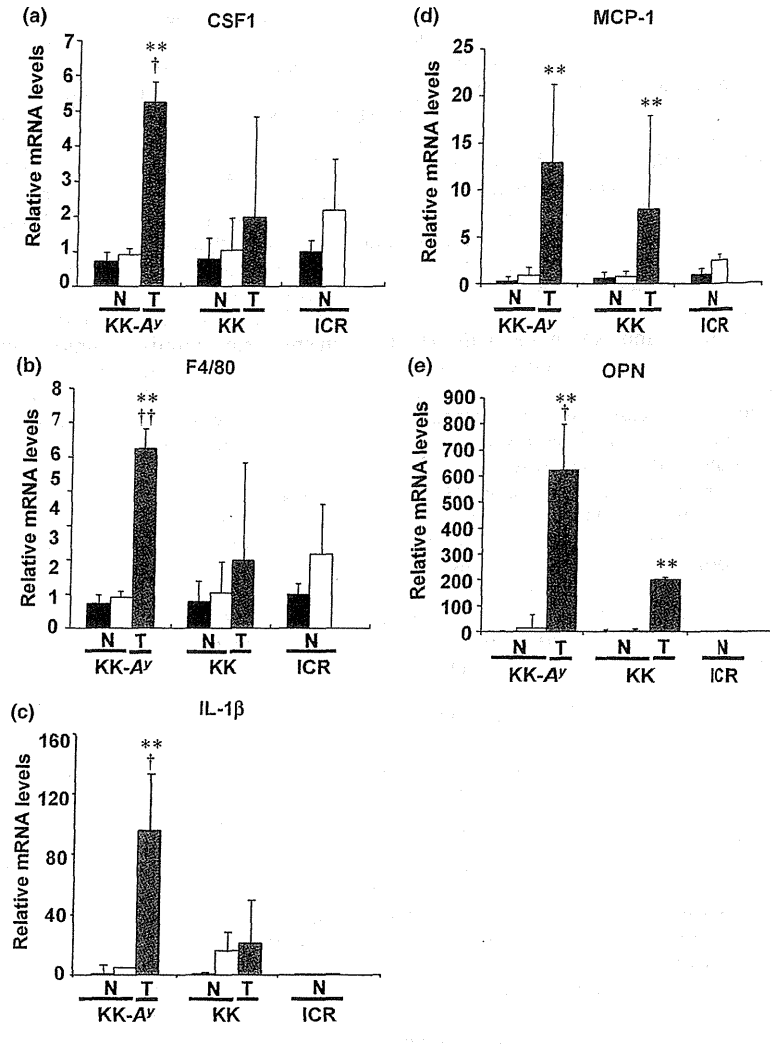

Fig. 7. Relative expression levels of mRNA regarding macrophage activation. Messenger RNA levels of colony-stimulating factor 1 (CSF1) (a), F4/80 (b), interleukin-1β (IL-1β) (c), monocyte chemotactic protein 1 (MCP1) (d), and osteopontin (OPN) (e) in non-cancerous (N) and cancerous (T) parts of colorectum in KK-A^y/TaJcl (KK-A^y), KK/TaJcl (KK), and ICR mice aged 25 weeks were examined by RT-PCR analysis. Data from the mucosa from the saline-treated group were set as 1. β-Actin mRNA level was used to normalize the data. ■, Mucosa from saline-treated group ($n = 3$); □, mucosa from azoxymethane-treated group ($n = 2$–4); ▨, cancerous part ($n = 5$–6). Data are mean ± SD. $^{**}P < 0.01$ *vs* tumor tissue from KK/TaJcl (KK) mice. $^{\dagger}P < 0.05$, $^{\dagger\dagger}P < 0.01$ *vs* mucosa from saline-treated group.

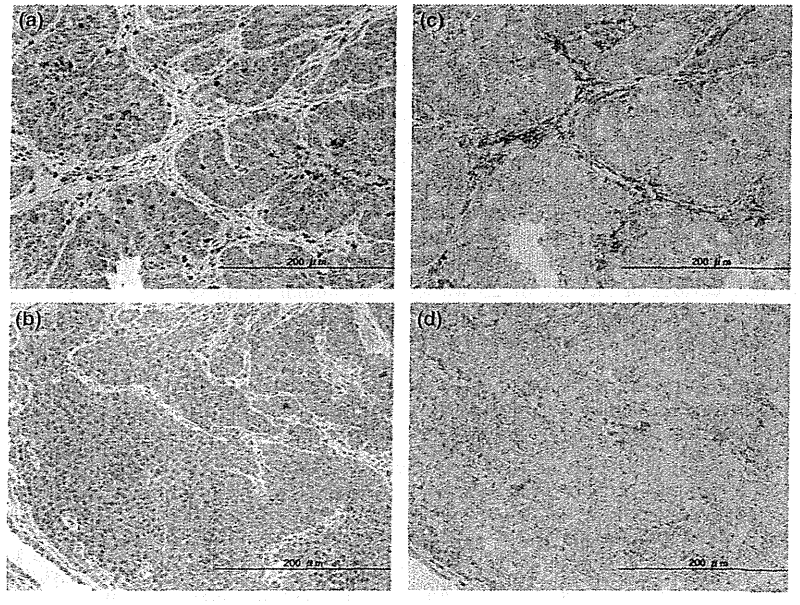

Fig. 8. Accumulation of macrophages in the colon tumor tissue of KK-A^y/TaJcl (KK-A^y) mice. Representative examples of colorectal cancer tissue immunostained with anti-colony-stimulating factor 1 antibodies (a,b) and anti-F4/80 antibodies (c,d) of KK-A^y (a,c) and KK/TaJcl (KK) (b,d) mice are shown. Bar = 200 μm.

18 Takayama T, Ohi M, Hayashi T *et al.* Analysis of K-ras, APC, and beta-catenin in aberrant crypt foci in sporadic adenoma, cancer, and familial adenomatous polyposis. *Gastroenterology* 2001; **121**: 599–611.
19 Kukitsu T, Takayama T, Miyanishi K *et al.* Aberrant crypt foci as precursors of the dysplasia-carcinoma sequence in patients with ulcerative colitis. *Clin Cancer Res* 2008; **14**: 48–54.
20 Mori H, Hata K, Yamada Y *et al.* Significance and role of early-lesions in experimental colorectal carcinogenesis. *Chem Biol Interact* 2005; **155**: 1–9.
21 Tetsu O, McCormick F. Beta-catenin regulates expression of cyclin D1 in colon carcinoma cells. *Nature* 1999; **398**: 422–6.
22 Araki Y, Okamura S, Hussain SP *et al.* Regulation of cyclooxygenase-2 expression by the Wnt and ras pathways. *Cancer Res* 2003; **63**: 728–34.
23 He W, Tan R, Dai C *et al.* Plasminogen activator inhibitor-1 is a transcriptional target of the canonical pathway of Wnt/beta-catenin signaling. *J Biol Chem* 2010; **285**: 24665–75.
24 Zins K, Abraham D, Sioud M, Aharinejad S. Colon cancer cell-derived tumor necrosis factor-alpha mediates the tumor growth-promoting response in macrophages by up-regulating the colony-stimulating factor-1 pathway. *Cancer Res* 2007; **67**: 1038–45.
25 Rao G, Wang H, Li B *et al.* Reciprocal interactions between tumor-associated macrophages and CD44 positive cancer cells via osteopontin/CD44 promote tumorigenicity in colorectal cancer. *Clin Cancer Res* 2013; **19**: 785–97.
26 Green CE, Liu T, Montel V *et al.* Chemoattractant signaling between tumor cells and macrophages regulates cancer cell migration, metastasis and neovascularization. *PLoS ONE* 2009; **8**: e6713.
27 Kaler P, Augenlicht L, Klampfer L. Macrophage-derived IL-1β stimulates Wnt signaling and growth of colon cancer cells; a crosstalk interrupted by vitamin D_3. *Oncogene*, 2009; **28**: 3892–902.
28 Kaler P, Galea V, Augenlichi L *et al.* Tumor associated macrophages protect colon cancer cells from TRAIL-induced apoptosis through IL-1β-dependent stabilization of Snail in tumor cells. *PLoS ONE*, 2010; **5**: e11700.
29 Kang J-C, Chen J-S, Lee C-H *et al.* Intratumoral macrophage counts correlate with tumor progression in colorectal cancer. *J Surg Oncol*, 2010; **102**: 242–8.

JJCO Japanese Journal of Clinical Oncology

Review Articles

Reprinted from

Jpn J Clin Oncol 2013;43(7)685–694
doi:10.1093/jjco/hyt053
Advance Access Publication 23 April 2013

Prevention and Intervention Trials for Colorectal Cancer

Masami Komiya[1], Gen Fujii[1], Mami Takahashi[2], Masaaki Iigo[3] and Michihiro Mutoh[1,*]

[1]Division of Cancer Prevention Research, National Cancer Center Research Institute, [2]Central Animal Division, National Cancer Center Research Institute, Tokyo and [3]Department of Molecular Toxicology, Nagoya City University Graduate School of Medical Sciences, Nagoya, Japan

JJCO Japanese Journal of Clinical Oncology

Review Articles

Jpn J Clin Oncol 2013;43(7)685–694
doi:10.1093/jjco/hyt053
Advance Access Publication 23 April 2013

Prevention and Intervention Trials for Colorectal Cancer

Masami Komiya[1], Gen Fujii[1], Mami Takahashi[2], Masaaki Iigo[3] and Michihiro Mutoh[1,*]

[1]Division of Cancer Prevention Research, National Cancer Center Research Institute, [2]Central Animal Division, National Cancer Center Research Institute, Tokyo and [3]Department of Molecular Toxicology, Nagoya City University Graduate School of Medical Sciences, Nagoya, Japan

*For reprints and all correspondence: Michihiro Mutoh, Division of Cancer Prevention Research, National Cancer Center Research Institute, 5-1-1, Tsukiji, Chuo-ku, Tokyo 104-0045, Japan. E-mail: mimutoh@ncc.go.jp

Received December 26, 2012; accepted March 20, 2013

There have been a number of candidates for chemopreventive agents from synthetic drugs and natural compounds suggested to prevent colorectal cancer. However, they have shown modest efficacy in humans. The reason for this could be partly explained by the use of inappropriate models *in vitro* and *in vivo,* and the limitation of chemoprevention trials. In Japan, there are no cancer chemopreventive medicines, and few cancer chemoprevention trials to date. In contrast, an increase in the prevalence of colorectal cancer in Japan has forced us to develop more efficient chemopreventive strategies. It is now a good time to review in detail the current status and future prospects for chemoprevention of colorectal cancer with respect to the future development of chemopreventive medicines, particularly using synthetic drugs and natural compounds in Asian populations. The role and mode of action of available synthetic drugs, mainly aspirin and metformin, are reviewed. In addition, the possible impact of natural compounds with anti-inflammatory/immunosuppressive properties, such as ω3 polyunsaturated fatty acid and lactoferrin, are also reviewed.

Key words: chemoprevention – aspirin – metformin – ω6-PUFAs – lactoferrin

INTRODUCTION

The prevalence of colorectal cancer (CRC) is increasing in Asia, including Japan, believed to be caused by changing dietary habits and lifestyle, interacting with genetic characteristics. Many Asian countries have experienced a 2- to 4-fold increase in CRC incidence over the past few decades (1). Fortunately, a natural history of sporadic CRC, evolution from normal mucosa to developing overt cancer, spans on average 10–20 years, thereby allowing us an opportunity for effective prevention and intervention. CRC can be prevented by lifestyle modification, i.e. taking regular physical activity, abstaining from smoking and taking healthy nutrition. Moreover, there are population screening methods for the early detection of CRC and adenomatous polyps, precursor lesions for CRC, such as using fecal occult blood testing and endoscopy. However, the efficacy of such screening and surveillance strategies for patient uptake is often suboptimal, limiting real effectiveness. Thus, there is a clear imperative to consider alternative preventative strategies, such as using cancer chemopreventive agents.

In contrast to 'chemotherapy', the term 'chemoprevention' was first introduced by Sporn (2). Chemoprevention is now defined as the use of specific agents, including natural and chemical compounds, to suppress, delay or reverse carcinogenesis, and thereby to prevent the development of cancers (3). As the user of cancer chemopreventive agents is not a cancer patient, the ideal cancer chemopreventive agent needs to meet several criteria: (i) it should have a convenient dosing schedule; (ii) it should be easily administered; (iii) it should be low cost; and most importantly; (iv) it should have very low side effects.

Subjects adopted for cancer chemopreventive trials are general populations or those who are in cancer high-risk

groups. Generally speaking, it is considered that patients in cancer high-risk groups, that is well-defined and representative for common CRC, are suitable subjects. Two conditions fall under this consideration, i.e. familial adenomatous polyposis (FAP) and Lynch syndrome. FAP is a rare autosomal dominant inherited disorder due to *APC* gene mutation, characterized by the occurrence of many polyps in the colorectum and other parts of the intestine. It has been reported that half of the patient population develops adenocarcinoma from intestinal polyps by the age of 40 years (4). Lynch syndrome is also known as a hereditary non-polyposis colon cancer, carrying a breakdown in DNA mismatch repair gene. Of note, there are other polyposis syndromes, but they are very rare and lack clear relevance to the general population, and hence not suitable as trial subjects. For instance, these are cases of juvenile polyposis, in which the responsible gene is *SMAD4*, Peutz–Jeghers syndrome, in which it is *STK11*, and Cowden syndrome, in which it is *PTEN*.

Based on reports of chemopreventive activity in the literature and/or efficacy data from *in vitro* models, animal models and human trials, the most promising drugs are aspirin and other non-steroidal anti-inflammatory drugs (NSAIDs). The effectiveness of these may be attributed to their potent inhibition of cyclooxygenase (COX) enzymes. In this review, important aspects of the current status and future prospects for chemoprevention of CRC, particularly using synthetic drugs (aspirin and metformin) and natural compounds (ω3 polyunsaturated fatty acid and lactoferrin), involving data of Asian populations, are summarized. Meanwhile, recent clinical trials have been requested to be registered in public trial registries (www.clinicaltrials.gov, www.actr.org.au, www.ISRCTN.org, www.umin.ac.jp/ctr/index/htm or www.trialregister.nl) so that anyone can obtain updated trial records in the database after the publication of this review.

CHEMICAL COMPOUNDS

Aspirin

A large number of epidemiological and experimental studies have indicated that NSAIDs reduce the risk of CRC. As COX-2 expression and prostaglandin (PG) E_2 synthesis is elevated in CRC, PGE_2 is more likely to enhance colorectal carcinogenesis than other prostanoids. The COXs/PGH synthases have two enzymes, COX-1 and COX-2, which catalyze both oxidative and reductive reactions in the PG synthesis pathway. The constitutive enzyme COX-1 is detectable, but has low expression in normal human colorectal tissue, whereas for the inducible enzyme COX-2, its expression is elevated under conditions of inflammation and cancer.

Aspirin is a conventional NSAID, and irreversibly inhibits COX-1 and COX-2, through selective acetylation of a specific serine residue of Ser^{529} and Ser^{516}, respectively (5). Low-dose aspirin (70–100 mg/day) is widely used for cardiovascular disease prevention. Aspirin has a short half-life (~20 min) and it preferentially inhibits platelet COX-1 in the presystemic circulation when administered at low doses once a day. Moreover, aspirin is a medicine that has been in use for a long time and its adverse events are well-defined; it meets all the criteria of chemopreventive agents, and thus has become the most widely studied pharmacological agent for the prevention of CRC.

Observational Studies

Kune et al. (6) first reported in humans that there is an inverse association between use of aspirin and the risk of CRC, in a study conducted in Australia. They investigated the relationship between risk of CRC and several chronic illnesses in 715 CRC cases and 727 age/sex-matched controls, and it was found that those who had used aspirin-containing medications in the past were less likely to develop CRC (relative risk, RR = 0.53, 95% confidence interval, CI 0.40–0.71). Moreover, a prospective cohort study (7) was conducted in the USA with 47 900 middle-aged male health professionals, who responded to a mailed questionnaire in 1986. The questionnaires aimed to assess the use of aspirin and other variables, including the occurrence of cancer in 1986, 1988 and 1990; 251 new patients were diagnosed with CRC during the study period. Regular users of aspirin (≥2/week) in 1986 had a lower risk of total CRC (RR = 0.68, CI 0.52–0.92). A meta-analysis of the case–control studies, on available data on the association between aspirin use and CRC by 2007 that included 20 815 cases of CRC, revealed that there was significantly lower use of aspirin or NSAIDs in cases than in control studies (8). These results support the contention that regular use of aspirin decreases the risk of CRC.

Randomized Controlled Trials

Observational studies can powerfully identify causal associations, but much has been learned from intervention trials. Reports of the randomized controlled trials of aspirin, such as APACC (9), AFPPS (10), CALGB (11) and ukCAP (12), revealed that aspirin (75–325 mg/day for 3 years) reduces the risk of any recurrent colorectal adenoma by 17% and advanced adenoma by 28% (13) (Table 1). Moreover, meta-analysis of aspirin on the long-term risk of death due to CRC in randomized trials of aspirin vs control revealed that the use of aspirin for around 5 years reduces the incidence of and mortality due to CRC by 30–40% after 20 years of follow-up (14). In the case of trials in cancer high-risk patients, such as FAP (CAPP1 or J-FAPP study) and Lynch syndrome (CAPP2 study) patients, they also present evidence of the effectiveness of aspirin as shown below (Table 1).

CAPP1

The CAPP1 was a double-blind, randomized trial in FAP patients with four arms: aspirin for 600 mg/day plus matched